

2-1-2019

Development of Gelatin and Graphene-Based Nerve Regeneration Conduits Using 3D Printing Strategies for Electrical Transdifferentiation of Mesenchymal Stem Cells

Metin Uz

Iowa State University, metinuz@iastate.edu

Maxsam Donta


Iowa State University, msdonta@iastate.edu

Meryem Mededovic

Iowa State University

See next page for additional authors

Follow this and additional works at: https://lib.dr.iastate.edu/cbe_pubs

 Part of the [Biomaterials Commons](#), [Chemical Engineering Commons](#), [Molecular and Cellular Neuroscience Commons](#), and the [Molecular, Cellular, and Tissue Engineering Commons](#)

The complete bibliographic information for this item can be found at https://lib.dr.iastate.edu/cbe_pubs/359. For information on how to cite this item, please visit <http://lib.dr.iastate.edu/howtocite.html>.

This Article is brought to you for free and open access by the Chemical and Biological Engineering at Iowa State University Digital Repository. It has been accepted for inclusion in Chemical and Biological Engineering Publications by an authorized administrator of Iowa State University Digital Repository. For more information, please contact digirep@iastate.edu.

Development of Gelatin and Graphene-Based Nerve Regeneration Conduits Using 3D Printing Strategies for Electrical Transdifferentiation of Mesenchymal Stem Cells

Abstract

In this study, gelatin and graphene-based nerve regeneration conduits/scaffolds possessing tailored 3D microstructures and mechanical properties were fabricated using 3D printing. The effect of 3D conduit microstructure and mechanical properties along with the applied electrical stimuli on mesenchymal stem cell (MSCs) behavior and transdifferentiation into Schwann cell (SC)-like phenotypes were investigated. The results indicated that the gelatin conduits/scaffolds had favorable 3D microstructural and mechanical properties for MSC attachment and growth. Immunocytochemistry results demonstrated that the application of electrical stimuli through the conductive graphene within the gelatin-based 3D microstructure had a profound effect on the differentiation of MSCs to SC-like phenotypes and their paracrine activity. 80% of the cells exhibited SC marker staining, and the cells showed significantly enhanced nerve growth factor (NGF) secretion. These results suggest that the electrical stimuli applied within the 3D gelatin matrix enables enhanced differentiation and paracrine activity compared to transdifferentiation procedures involving electrical stimuli applied on 2D substrates and chemical stimuli applied in 3D gelatin scaffolds, leading to promising nerve regeneration strategies.

Disciplines

Biomaterials | Chemical Engineering | Molecular and Cellular Neuroscience | Molecular, Cellular, and Tissue Engineering

Comments

This document is the unedited Author's version of a Submitted Work that was subsequently accepted for publication in *Industrial & Engineering Chemistry Research*, copyright © American Chemical Society after peer review. To access the final edited and published work see DOI: [10.1021/acs.iecr.8b05537](https://doi.org/10.1021/acs.iecr.8b05537).

Authors

Metin Uz, Maxsam Donta, Meryem Mededovic, Donald S. Sakaguchi, and Surya Mallapragada

1
2
3 **Development of Gelatin and Graphene-Based Nerve Regeneration Conduits Using 3D**
4
5 **Printing Strategies for Electrical Transdifferentiation of Mesenchymal Stem Cells**
6

7 Metin Uz¹, Maxsam Donta¹, Meryem Mededovic¹, Donald S. Sakaguchi² and Surya

8
9 Mallapragada^{1*}
10

11 ¹ Chemical and Biological Engineering, Iowa State University

12
13 ² Genetics, Development and Cell Biology, Iowa State University
14
15
16
17
18
19

20 **Corresponding Author:*

21
22 *Surya Mallapragada, Department of Chemical and Biological Engineering, Iowa State University,*
23
24 *Ames, IA 50011*

25
26 *Email: suryakm@iastate.edu*

27
28 *Phone: 515-294-7407*

29
30 *Fax: 515-294-2689*
31
32
33
34
35
36
37
38
39
40
41
42
43
44
45
46
47
48
49
50
51
52
53
54
55
56
57
58
59
60

Abstract

In this study, gelatin and graphene-based nerve regeneration conduits/scaffolds possessing tailored 3D microstructures and mechanical properties were fabricated using 3D printing. The effect of 3D conduit microstructure and mechanical properties along with the applied electrical stimuli on mesenchymal stem cell (MSCs) behavior and transdifferentiation into Schwann cell (SC)-like phenotypes were investigated. The results indicated that the gelatin conduits/scaffolds had favorable 3D microstructural and mechanical properties for MSC attachment and growth. Immunocytochemistry results demonstrated that the application of electrical stimuli through the conductive graphene within the gelatin-based 3D microstructure had a profound effect on the differentiation of MSCs to SC-like phenotypes and their paracrine activity. 80% of the cells exhibited SC marker staining, and the cells showed significantly enhanced nerve growth factor (NGF) secretion. These results suggest that the electrical stimuli applied within the 3D gelatin matrix enables enhanced differentiation and paracrine activity compared to transdifferentiation procedures involving electrical stimuli applied on 2D substrates and chemical stimuli applied in 3D gelatin scaffolds, leading to promising nerve regeneration strategies.

Introduction

Large peripheral nerve injuries (PNIs) affect 13 to 23 out of every 100,000 people each year, leading to possible long-term disability, reduced quality of life, and heavy economic and social burdens.¹ Over 200,000 peripheral nerve repair procedures are performed annually, resulting in approximately \$150 billion spent in annual health-care dollars in the United States.² Currently autologous nerve graft-based treatment strategies are considered the gold standard, yet suffer from a number of limitations including the requirement of multiple surgeries, biological complexity, donor site morbidity, and lack of graft tissue; and are not able to facilitate satisfactory recovery.³ Schwann cells (SCs) and implantable nerve conduit-based therapies are a promising alternative; however, donor site morbidity, lack of availability and slow *in vitro* growth of SCs limit the clinical translation and potential positive outcomes of this strategy.⁵⁻⁹ Mesenchymal stem cells (MSCs), isolated and derived from various connective tissue sources, hold considerable potential for cell-based nerve regeneration therapies using autologous transplantation.^{10, 11} MSCs can be transdifferentiated *in vitro* into SC-like phenotypes with enhanced paracrine activity and can be used for peripheral nerve regeneration without any ethical concerns.¹²⁻²⁰ However, the current difficulties in providing scalable differentiation protocols, designing a cell-laden implantable conduit with desired 3D microstructural/mechanical properties that mimic the complex extracellular matrix (ECM) microenvironment, as well as difficulties in precise control of the final fate of the implanted cell population, limit the *in vivo* application and clinical use of MSCs for peripheral nerve regeneration.^{10, 20, 21} In addition, most of the currently applied *in vitro* transdifferentiation procedures rely on the use of expensive chemicals and growth factors without deep mechanistic understanding of regulated proteins and cellular pathways. Furthermore, these procedures are mostly tested on 2D substrates, which do not represent the natural 3D microenvironment of the cells.^{13, 14, 16, 20, 22} Therefore, the current knowledge of mechanisms of

1
2
3 transdifferentiation of MSCs in a controlled 3D microenvironment with tunable properties is
4 significantly limited and should be expanded with alternative approaches.
5
6
7

8
9 In our previous study, we have successfully transdifferentiated MSCs into SCs with enhanced
10 paracrine activity in the 3D microstructure of gelatin-based conduits via chemical induction.²³ We
11 have also recently demonstrated the transdifferentiation of MSCs into SCs via electrical stimuli
12 on conductive graphene-based 2D substrates.²⁴ Based on this background, here we propose 3D
13 bioprinted gelatin and graphene-based conductive, biodegradable and implantable conduits with
14 desired microstructural/mechanical properties, mimicking the ECM microenvironment for *in vitro*
15 and potential *in vivo* transdifferentiation of MSCs into SCs and *in vivo* peripheral nerve
16 regeneration via electrical stimuli. We hypothesize that the synergistic effect of 3D
17 microstructural/mechanical conduit properties combined with electrical stimuli will enhance
18 transdifferentiation of MSCs into SCs. We rationalize that the tunable 3D gelatin conduit
19 microstructure will provide the desired ECM microenvironment for cellular attachment, growth,
20 differentiation and paracrine activity, while the graphene circuit embedded in the gelatin matrix
21 via 3D printing will enable conductivity and *in vitro* and potential *in vivo* differentiation via electrical
22 stimuli. The overall objective of this study is to overcome the current challenges of *in vitro* stem
23 cell differentiation and enable potential *in vivo* applications, which will then open the way for an
24 ultimate goal of creating effectively applicable clinical PNI repair strategies via the proposed
25 conduit design.
26
27
28
29
30
31
32
33
34
35
36
37
38
39
40
41
42
43
44
45
46

47 **Materials and Methods**

48 **Preparation of Gelatin Conduits with Graphene Rods**

49
50 Gelatin conduits were prepared by combining molding and thermally induced phase separation
51 (TIPS) techniques, as described in our previous work.²³ Briefly, the mold was first assembled by
52 inserting a conductive graphene rod (3.0 mm in diameter) (Black Magic 3D) into a Teflon tube (5
53
54
55
56
57
58
59
60

1
2
3 mm in diameter). The dimensions of the conduits and the integrated graphene rods can be
4
5 adjusted by changing the mold and graphene rod diameters. Gelatin (Type B gelatin from bovine
6
7 skin, Sigma) solution was prepared by dissolving 0.5 g gelatin in 10 mL of deionized water at 55
8
9 °C. Then, the gelatin solution was injected into the mold. The molds with gelatin were kept at -20
10
11 °C for 5 h for phase separation and incubated in cold ethanol (-18 °C) overnight. After that, the
12
13 graphene integrated gelatin was removed from the mold, incubated in nonsolvent, 1, 4-dioxane,
14
15 for 2 days and freeze-dried overnight. The obtained gelatin-graphene conduits were cross-linked
16
17 using 1-ethyl-3-(3-dimethyl-aminopropyl) carbodiimide HCl (EDC) and N-hydroxy-succinimide
18
19 (NHS) chemistry.²³
20
21
22
23

24 **Preparation of 3D Printed Graphene Circuits Integrated Gelatin Scaffolds**

25
26 A conductive graphene PLA filament (Black Magic 3D) was used to 3D print the interdigitated
27
28 circuit with desired dimensions. The CAD model of the designed interdigitated circuit was
29
30 configured in Slic3r software to adjust printing parameters and continuous 3D deposition of
31
32 computer-designed circuit was performed using a filament-based 3D printer (LulzBot TAZ 6). After
33
34 fabrication, the graphene-based interdigitated circuit was embedded in a gelatin solution that had
35
36 been prepared as described above. Then, the same scaffold formation and cross-linking steps
37
38 were followed as described above.
39
40
41
42

43 **Characterization of Conduits/Scaffolds**

44
45 The 3D microstructure (pore size and % porosity) of conduits/scaffolds were observed via
46
47 scanning electron microscopy (SEM, make and model of SEM?). The mechanical properties of
48
49 the conduits/scaffolds were detected via dynamic mechanical analyzer (DMA). The swelling ratio
50
51 was determined by measuring the weight of the conduits/scaffolds before and after dipping them
52
53 in deionized water. The conductivity of integrated circuits was tested by building up a circuit to
54
55 light a bulb and measuring the resistance.
56
57
58
59
60

Cell Culture of MSCs

Previously isolated Brown Norway rat MSCs^{25, 26} were grown in minimum essential medium (α -MEM, Gibco BRL) supplemented with 20% fetal bovine serum (FBS; Atlanta Biologicals), 4 mM l-glutamine (Gibco), and antibiotic-antimycotic (Invitrogen)(this growth medium is referred to as maintenance medium, MM) and incubated at 37 °C and 5% CO₂ environment. The cells were sub-cultured when they reached 80% confluence, every 2–3 days.

Cellular Attachment and Growth

The MSCs were seeded (5×10^5 cells) to the conduits/scaffolds to evaluate their cellular attachment and growth within the conduit matrix. The cells were injected as a suspension via micropipet within the conduit matrix and incubated for 15 days at 37 °C and 5% CO₂ environment by changing the cell culture media every 2 days. During the incubation, cell viability, proliferation and growth was observed. After the incubation, the cells were fixed in 4% paraformaldehyde and labelled with Rhodamine Phalloidin and DAPI to detect the cellular morphology, proliferation, and interconnection within the 3D conduits.

Transdifferentiation

Rat MSCs were transdifferentiated *in vitro* into SC-like phenotypes using electrical stimuli, by following the previously mentioned protocols.²⁴ MSCs (5×10^5 cells) seeded in either gelatin conduits integrated with graphene rods, or the gelatin scaffolds with graphene-based interdigitated circuits embedded within. Then, the cells were grown within the conduit microstructures for 1-2 days. Following this, an electrical potential of 100 mV at 50 Hz was applied for 2 min per day for 10 days through the rod, while the same electrical potential was applied to the interdigitated circuit for 10 min per day for 10 days to transdifferentiate MSCs into SCs. These

1
2
3 electrical parameters were selected based on our previous studies and the electrical signals and
4 fields occurring endogenously during embryonic development.²⁰ MSCs (5×10^5 cells) seeded in
5 the conduits/scaffolds and incubated in MM for 10 days without electrical transdifferentiation were
6 used as controls.
7
8
9
10

11 12 13 **Immunocytochemistry**

14
15 The degree of transdifferentiation was evaluated by immunocytochemistry analysis using glial cell
16 markers, calcium binding protein Rabbit- α -S100, Mouse- α -S100 β (Abcam-ab11178), and low-
17 affinity neurotrophin receptor Rabbit- α -p75 (Promega-G3231). The control and transdifferentiated
18 MSCs within the conduit/scaffold microstructures were fixed in 4% paraformaldehyde. After
19 washing with phosphate buffered saline (PBS), the cells were incubated with blocking buffer (5%
20 normal donkey serum (NDS, Jackson ImmunoResearch, West Grove, PA, USA), 0.4% bovine
21 serum albumin (BSA; Sigma) and 0.2% Triton X-100 (Fisher Scientific) in PBS) for one hour.
22 Then, the primary antibodies of Rabbit- α -S100, Mouse- α -S100 β and Rabbit- α -p75 (1:500) were
23 applied to the samples and incubated at 4 °C overnight. The next day, the samples were washed
24 with PBS and labelled with corresponding secondary antibodies, Donkey- α -Mouse-Cy3 (1:500,
25 Jackson ImmunoResearch), Donkey- α -Rabbit-Cy3 (1:500, Jackson ImmunoResearch), and
26 DAPI (4',6-diamidino-2-phenylindole) (1:2000, Invitrogen) (for nuclei staining) in blocking buffer.
27 After 90 min of incubation in the dark at room temperature, the samples were rinsed with PBS
28 and fluorescence microscopy imaging was performed.
29
30
31
32
33
34
35
36
37
38
39
40
41
42
43
44
45
46

47 **ELISA Test**

48
49 The paracrine activity of the MSCs during the transdifferentiation process was also evaluated
50 using specific ELISA test kits. Since SCs are known to secrete high amounts of nerve growth
51 factor (NGF) upon injury, we primarily analyzed NGF secretion. During the transdifferentiation,
52 cell culture media was collected every 2 days and the amount of NGF secreted was detected
53
54
55
56
57
58
59
60

1
2
3 through the corresponding ELISA kit (Abcam Rat Beta NGF ELISA kit ab100757) by following the
4 manufacturer's protocol.
5

6 7 **Co-culture with PC12-TrkB Cells**

8
9 A non-contact co-culture system was used to evaluate the biological activity of secreted factors
10 produced during the MSC transdifferentiation process. MSC (5×10^5 cells) laden gelatin scaffolds
11 with graphene-based interdigitated circuits were co-cultured with PC12-TrkB cells²⁷ (provided by
12 Dr. Moses Chao, Helen L. and Martin S. Kimmel Center for Biology and Medicine at the Skirball
13 Institute for Biomolecular Medicine, New York Univ.) using non-contact trans-well plates (Corning
14 transwell inserts Product #3412). The scaffolds with MSCs were placed onto the 0.4 μm pore size
15 cell inserts, which were then placed above the PC12-TrkB cells seeded into 6-well plates. The
16 co-culture media was composed of 70% PC12 cell culture media (RPMI-1640 supplemented with
17 10% equine serum and 5% FBS) and 30% of MM. During the co-culture, an electrical stimulus
18 (100 mV at 50 Hz, 10 min per day for 10 days) was applied only to the MSCs seeded in the
19 scaffolds. At the end of this incubation, the extent of neurite outgrowth from the PC12-TrkB cells
20 was visualized under fluorescence microscopy after ICC analysis using primary antibody Tuj1
21 and secondary Alexa Fluor 488 (1:1000, Molecular Probes-Life Technologies, Carlsbad, CA,
22 USA).
23
24
25
26
27
28
29
30
31
32
33
34
35
36
37
38
39
40

41 **Results and Discussion**

42 **Characterization of Fabricated Conduit/Scaffold**

43
44 In this, study, we successfully developed conductive gelatin conduits with integrated graphene
45 rods (**Figure 1 A**) and gelatin scaffolds with embedded 3D printed graphene-based interdigitated
46 circuits (**Figure 1 B**). The image of graphene interdigitated circuit embedded in gelatin after 3D
47 printing can be seen in **Figure 1 B**. The graphene rods and interdigitated circuits were completely
48 solid and intact, surrounded with the gelatin conduit/scaffold. The graphene rods and
49 interdigitated circuits had a resistance of ~ 50 k Ω and were conductive enough to light a LED bulb
50
51
52
53
54
55
56
57
58
59
60

(Figure 1 A and B). The gelatin conduit and scaffolds surrounding the graphene rods and interdigitated circuits had similar microstructure as seen in SEM images presented in Figure 1 A and B. These microstructures had 90% porosity with the average pore size of $\sim 135 \mu\text{m}$. These structures also underwent swelling when they were in contact with water and the swelling ratio was calculated as 830. The obtained conduits microstructures showed similarity with our previous work²³ since we applied same fabrication method. Therefore, the integration of graphene-based rods or 3D graphene circuits did not affect the conduit/scaffold structure.

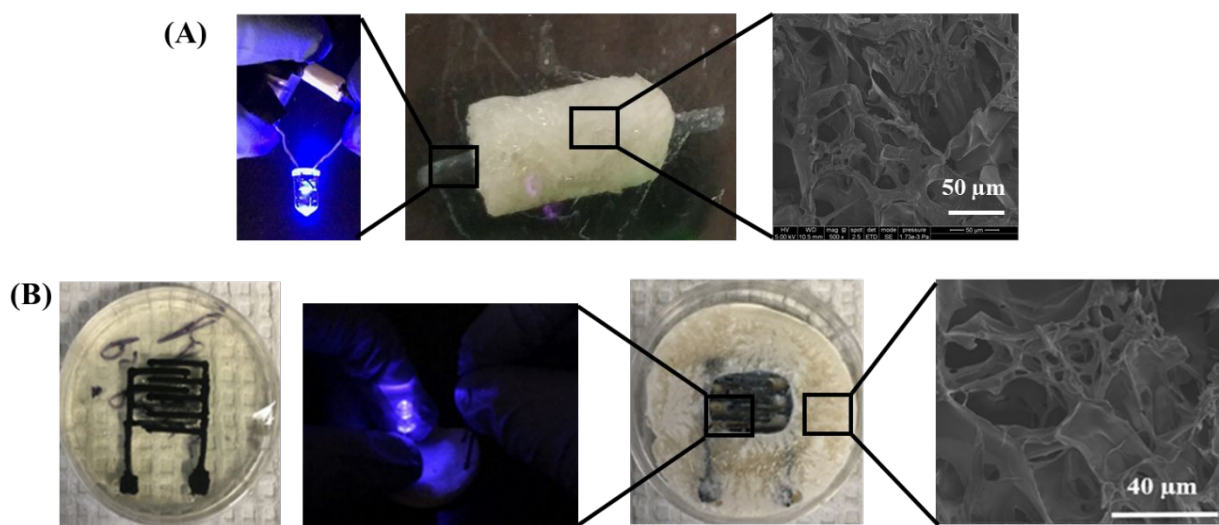


Figure 1. (A) Graphene rod integrated gelatin conduits. (B) Graphene-based interdigitated circuit embedded gelatin scaffold.

In addition to the microstructural properties, the mechanical features of the conduits/scaffolds were also evaluated. During this evaluation, the integrated solid graphene rods and circuits were not included and only the mechanical properties of gelatin-based structure was evaluated. The gelatin structure displayed an elastic behavior with storage modulus (G') higher than the loss modulus (G'') as shown in Figure 2 A and B. In addition, the G' and G'' values remained independent of the strain amplitude confirming the linear viscoelastic behavior (Figure 2 A). The average complex modulus (G^* , a measure of the stiffness) was calculated as $7.6 \times 10^6 \text{ Pa}$ (at a

frequency of 0.1 Hz, using 0.1% strain) while the loss factor ($\tan \delta$, a measure of the internal energy dissipation) was calculated as 0.11. Since G' value was higher than the G'' , the storage modulus (G') dominated the complex modulus (G^*). These results indicated that the gelatin structure depicted an elastic behavior while exhibiting solid-like behavior at physiological temperatures ($0 < \tan \delta < 1$). The typical stress-strain curve of the gelatin scaffolds was also measured (**Figure 2 C**). The results indicated that the Young's modulus of the gelatin scaffolds was around 80 MPa with a yield strength of ~ 1.8 MPa, showing elastic behavior.

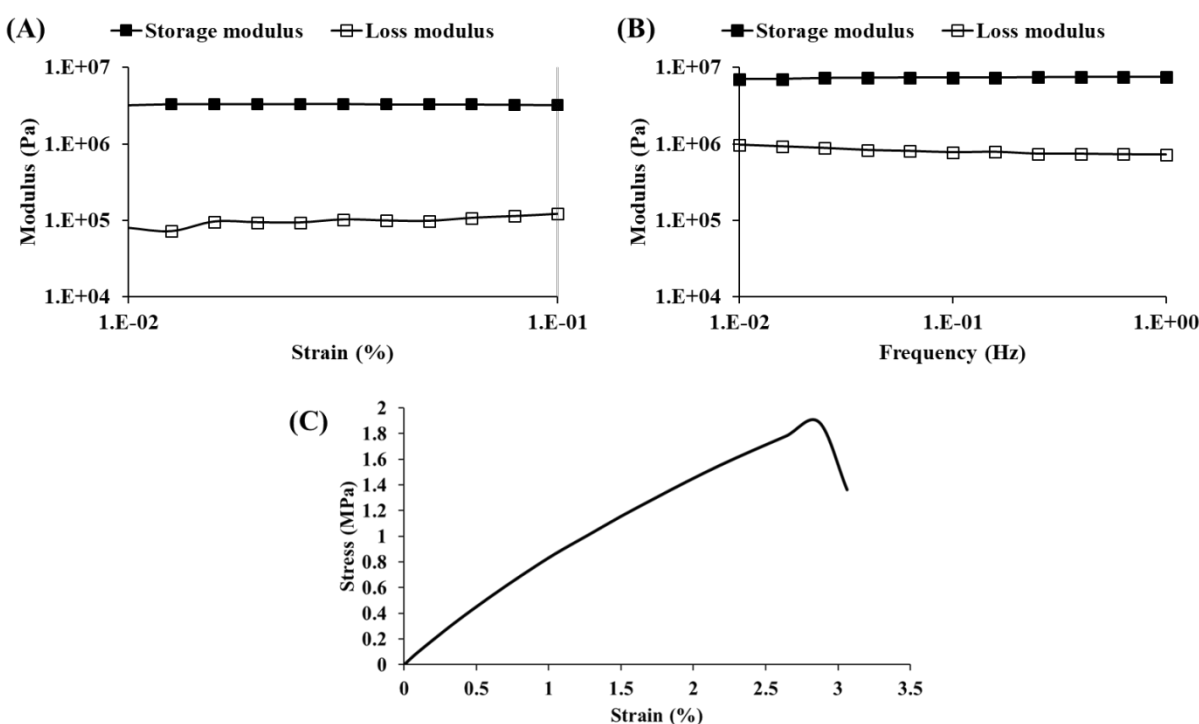


Figure 2. The storage (G') and loss (G'') moduli, as a function of **(A)** percent strain and **(B)** frequency. **(C)** Stress-strain curve of the gelatin scaffolds.

Cellular Growth and Differentiation of MSCs in the Conduit/Scaffold

The material-cell interactions were observed by seeding the MSCs in the gelatin structure. It was noted that the MSCs can attach, grow and proliferate within the 3D microstructure of gelatin matrix for more than 15 days without any issue of cell viability (**Figure 3**). It was also observed that MSCs

1
2
3 created a 3D intercellular network within the porous 3D microstructure (**Figure 3 B**). It is known
4 that gelatin is a favorable material for cell attachment and growth. In addition, the 3D structure,
5 pore size, porosity, mechanical elasticity and swelling property of the gelatin matrix has a
6 profound effect on cell attachment and growth. The heterogeneous and anisotropic 3D structure
7 can contribute to the recruitment of proteins to adhesion sites, which may also facilitate
8 proliferation and spreading.²⁸⁻³⁰ Matrix stiffness can also have an influence on the attachment,
9 growth and differentiation along with the intrinsic mechanical properties of the cells as depicted in
10 previous studies.³¹⁻³³ Together, these factors create a favorable microenvironment, mimicking the
11 natural extracellular matrix, for MSCs.
12
13
14
15
16
17
18
19
20
21
22
23

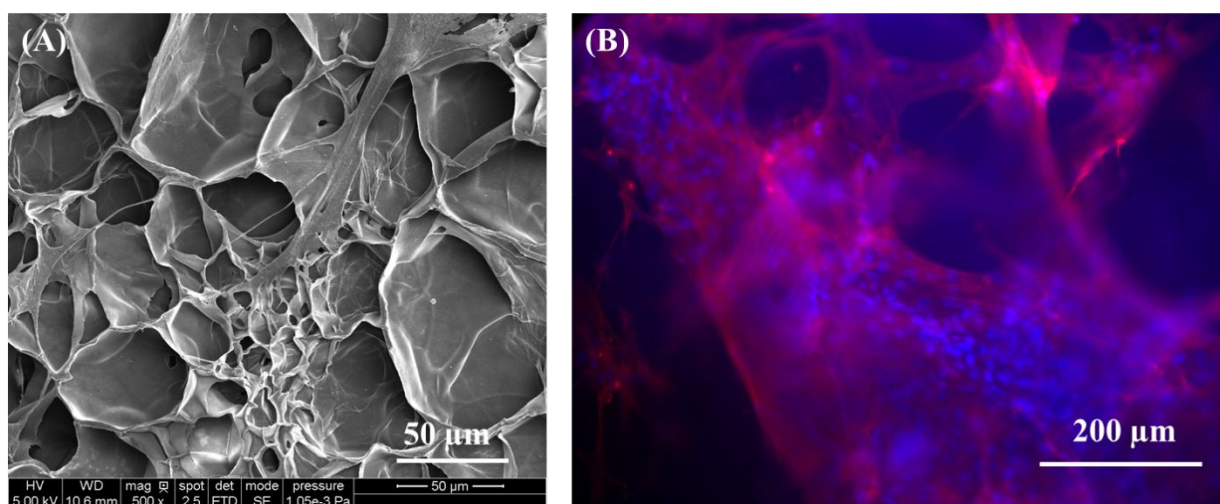
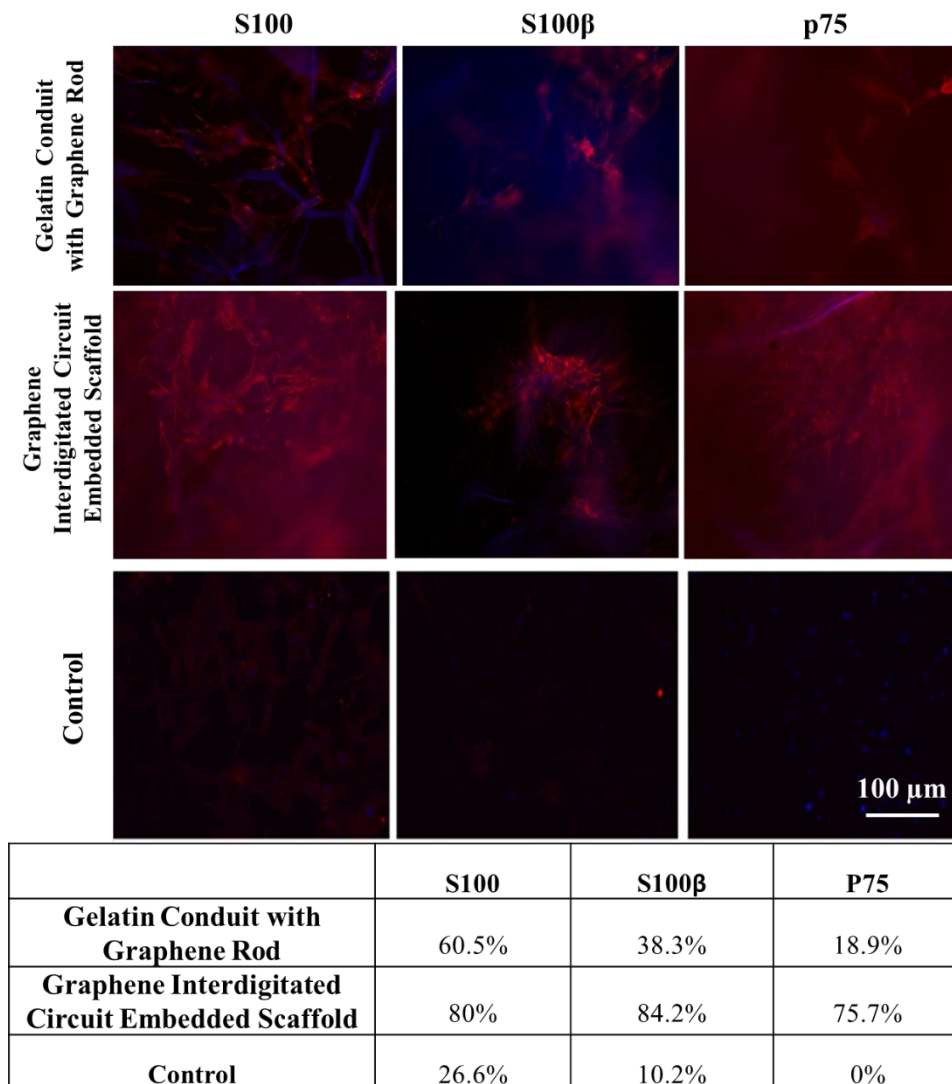


Figure 3. MSCs attachment, growth and proliferation within gelatin matrix. **(A)** SEM image. **(B)** Fluorescence image of Rhodamine phalloidin (red) and DAPI staining of MSCs within the gelatin scaffold. Scale bar in B, 200 μm .

The application of electrical stimuli within the favorable 3D gelatin microstructure resulted in enhanced differentiation of MSCs into SC-like phenotypes due to the synergistic effect of 3D microstructural/mechanical cues and electrical stimuli. We conducted an ICC analysis using s100, s100 β and P75 antibodies as SC-markers considering the reports indicating their expression in

1
2
3 Schwann cells and regulation during injury and differentiation.^{34, 35, 36} The ICC results indicated
4 that MSCs seeded in the gelatin conduits with integrated graphene rods showed low degree of
5 differentiation with 60% immunolabeling of S100, 38% immunolabeling of S100 β and 18%
6
7 immunolabeling of P75 SC-markers (**Figure 4, first row**). This could be attributed to the electric
8
9 field created in the gelatin matrix through the conductive graphene rod not being strong enough
10
11 to support robust transdifferentiation. Considering this, we replicated the interdigitated circuit
12
13 geometry from our previous work²⁴ on flat substrates, with different dimensions in the gelatin
14
15 conduits using 3D printing. The ICC results showed that the MSCs, seeded in the gelatin scaffolds
16
17 with 3D printed graphene interdigitated circuits, demonstrated significantly higher degrees of
18
19 differentiation with 80% immunolabelling of S100, 84% immunolabeling of S100 β and 75%
20
21 immunolabeling of P75 SC-markers (**Figure 4, second row**). This result is comparable to our
22
23 previous studies where we transdifferentiated MSCs into SCs within a 3D gelatin structure using
24
25 chemical induction, and obtained a degree of transdifferentiation of around 85%.²³ In another
26
27 study from our group, we used 2D inkjet printed graphene interdigitated circuits on non-
28
29 degradable polyimide substrates to transdifferentiate MSCs into SCs using electrical induction.
30
31 The degree of transdifferentiation achieved with this approach was also around 85%.²⁴ Here, by
32
33 combining the 3D microstructure and electrical stimuli, we were able to achieve around 80% of
34
35 degree of transdifferentiation with electrical stimuli in a 3D microstructured conduit, which
36
37 demonstrates the efficiency of our approach.
38
39
40
41
42

43 The transdifferentiation could potentially occur through promoting the upregulation of key neural
44
45 gene expression patterns associated with focal adhesion kinase (FAK) signaling or mitogen-
46
47 activated protein kinase signaling (p38) pathways³⁷⁻⁴² or via altering cellular membrane potential
48
49 through hyperpolarization and depolarization, modification of ion channels, activation of calcium
50
51 channels, and/or upregulation of the ERK pathway.⁴³⁻⁴⁵ Other potential mechanisms might be
52
53 through the activation of various signaling pathways such as MAPK, PI3K, and/or ROCK,^{46, 47}
54
55 and the increase in intracellular ROS generation.^{46, 48}
56
57
58
59
60



39 **Figure 4.** Transdifferentiation of MSCs in 3D conduits/scaffolds. MSCs in gelatin structure without
40 any stimuli was used as control. Glial cell markers: s100, S100β and p75. Staining with Red: Cy3
41 and Blue: DAPI. Cell density: 5×10^5 cells per sample.
42
43
44
45

46
47 Another indication of successful transdifferentiation is enhanced paracrine activity. Schwann cells
48 are known to secrete certain neurotrophic factors, particularly NGF, during injury that helps
49 myelination and supports axonal regeneration.^{14, 49} Considering this, we quantified the amount of
50 secreted NGF during the transdifferentiation process. Our results indicated that the amount of
51 NGF secreted from MSCs seeded in gelatin conduits with integrated graphene rods during
52
53
54
55
56
57

transdifferentiation was around 0.175 pg/mL per cell (**Figure 5 A**). This result was close to the control case and was expected, since the degree of differentiation obtained from ICC results for the MSCs in this conduit was also low. It is anticipated that this could be due to the insufficient electrical field created in the gelatin conduit using the conductive graphene rod. In contrast, the MSCs transdifferentiated within gelatin scaffolds with embedded 3D printed graphene interdigitated circuits, secreted NGF amounts of ~5 pg/mL per cell, which is significantly higher than the other counterpart and control groups (**Figure 5 A**). In addition, this was also found to be considerably higher than the NGF secretion obtained in our previous studies, which varied between 0.5 to 2.5 pg/mL per cell.^{23, 24} Therefore, the synergistic effect of 3D microstructural and mechanical properties and electrical stimuli did not cause significant measurable improvements in the degree of differentiation; however, it significantly enhanced the paracrine activity. To further demonstrate the biological activity of the secreted NGF, we conducted a non-contact co-culture experiment with PC12-TrkB cells. The results indicated a significant extension in the PC12-TrkB cells neurites, calculated as 5 μm per cell, obtained when the PC12-TrkB cells were in co-culture with MSCs seeded in gelatin scaffolds with embedded 3D printed graphene interdigitated circuits exposed to electrical stimuli (**Figure 5 B**). The control cells displayed little to no neurite outgrowth.

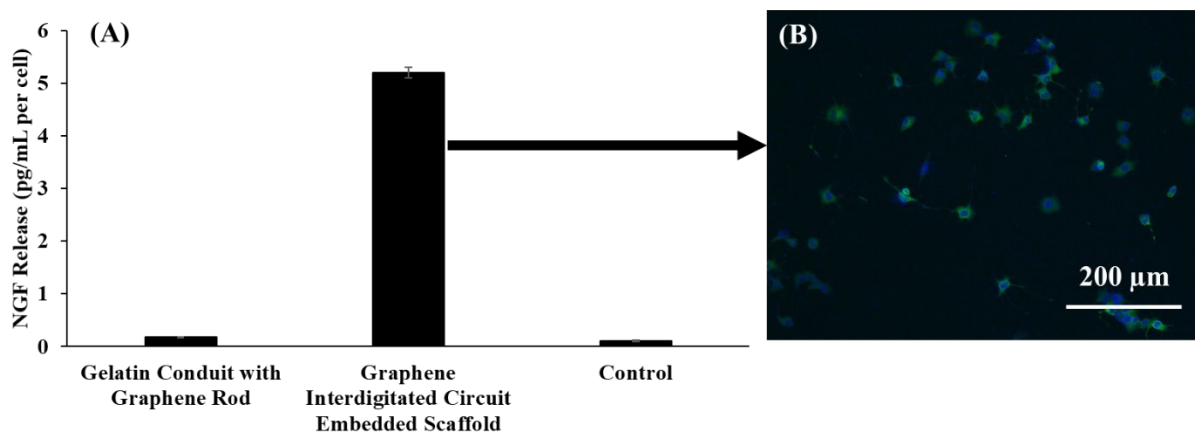


Figure 5. (A) Paracrine activity of MSCs differentiated in 3D conduits/scaffolds and secreted amounts of NGF. **(B)** Biological activity of secreted NGF on PC12-TrkB cells.

Conclusions

The synergistic use of 3D microstructural and mechanical cues in combination with electrical stimuli can be used as an alternative transdifferentiation strategy. This approach also eliminates the need for chemical stimuli-based conventional transdifferentiation protocols, which are non-scalable and potentially reversible, preventing direct *in vivo* application. Integration of 3D printed microcircuits within a scaffold structure can provide spatial and local control on cellular behavior. Moreover, this strategy can further be developed to enable potential *in situ-in vivo* control on the implanted cell population via electrical stimuli. The future direction will be to investigate different electrical stimuli parameters and obtain a clearer mechanistic understanding of electrical stimuli-based transdifferentiation. These results are promising and have potential to pave the way for alternative peripheral nerve regeneration strategies.

Acknowledgments

SKM would like to thank Prof. Juvekar for introducing her to the joys of research and for his excellent teaching and mentoring during her formative years. The authors would like to acknowledge the US Army Medical Research and Materiel Command under contract W81XWH-11-1-0700 and the Stem Cell Biology Fund for funding this work. SKM would also like to acknowledge support for this work from the Carol Vohs Johnson Chair. We also would like to thank Dr. Michael Bartlett and Ravi Tutika for helping with the tensile test measurements.

References

1. Muheremu, A.; Ao, Q., Past, Present, and Future of Nerve Conduits in the Treatment of Peripheral Nerve Injury. *BioMed. Res. Int.* **2015**, 2015, 6.
2. Grinsell, D.; Keating, C. P., Peripheral Nerve Reconstruction after Injury: A Review of Clinical and Experimental Therapies. *BioMed. Res. Int.* **2014**, 2014, 13.
3. Gu, X., Progress and perspectives of neural tissue engineering. *Front. Med.* **2015**, 9, 401-411.
4. Gu, X.; Ding, F.; Williams, D. F., Neural tissue engineering options for peripheral nerve regeneration. *Biomater.* **2014**, 35, 6143-6156.

5. Guenard, V.; Kleitman, N.; Morrissey, T. K.; Bunge, R. P.; Aebischer, P., Syngeneic Schwann cells derived from adult nerves seeded in semipermeable guidance channels enhance peripheral nerve regeneration. *J. Neurosci.* **1992**, *12*, 3310-20.
6. Mosahebi, A.; Fuller, P.; Wiberg, M.; Terenghi, G., Effect of allogeneic Schwann cell transplantation on peripheral nerve regeneration. *Exp. Neurol.* **2002**, *173*, 213-23.
7. Mosahebi, A.; Woodward, B.; Wiberg, M.; Martin, R.; Terenghi, G., Retroviral labeling of Schwann cells: in vitro characterization and in vivo transplantation to improve peripheral nerve regeneration. *Glia* **2001**, *34*, 8-17.
8. Rodriguez, F. J.; Verdu, E.; Ceballos, D.; Navarro, X., Nerve guides seeded with autologous schwann cells improve nerve regeneration. *Exp. Neurol.* **2000**, *161*, 571-84.
9. Rutkowski, G. E.; Miller, C. A.; Jeftinija, S.; Mallapragada, S. K., Synergistic effects of micropatterned biodegradable conduits and Schwann cells on sciatic nerve regeneration. *J. Neural Eng.* **2004**, *1*, 151-7.
10. Morrison, S. J.; Spradling, A. C., Stem Cells and Niches: Mechanisms That Promote Stem Cell Maintenance throughout Life. *Cell* **2008**, *132*, 598-611.
11. Sandquist, E. J.; Uz, M.; Sharma, A. D.; Patel, B. B.; Mallapragada, S. K.; Sakaguchi, D. S., Stem Cells, Bioengineering, and 3-D Scaffolds for Nervous System Repair and Regeneration. In *Neural Engineering*, Springer: 2016, 25-81.
12. Brohlin, M.; Mahay, D.; Novikov, L. N.; Terenghi, G.; Wiberg, M.; Shawcross, S. G.; Novikova, L. N., Characterisation of human mesenchymal stem cells following differentiation into Schwann cell-like cells. *Neurosci. Res.* **2009**, *64*, 41-9.
13. Dezawa, M.; Takahashi, I.; Esaki, M.; Takano, M.; Sawada, H., Sciatic nerve regeneration in rats induced by transplantation of in vitro differentiated bone-marrow stromal cells. *Eur. J. Neurosci.* **2001**, *14*, 1771-6.
14. Keilhoff, G.; Goihl, A.; Stang, F.; Wolf, G.; Fansa, H., Peripheral nerve tissue engineering: autologous Schwann cells vs. transdifferentiated mesenchymal stem cells. *Tissue Eng.* **2006**, *12*, 1451-65.
15. Ladak, A.; Olson, J.; Tredget, E. E.; Gordon, T., Differentiation of mesenchymal stem cells to support peripheral nerve regeneration in a rat model. *Exp. Neurology* **2011**, *228*, 242-252.
16. Sharma, A. D.; Zbarska, S.; Petersen, E. M.; Marti, M. E.; Mallapragada, S. K.; Sakaguchi, D. S., Oriented growth and transdifferentiation of mesenchymal stem cells towards a Schwann cell fate on micropatterned substrates. *J. Biosci. Bioeng.* **2016**, *121*, 325-35.
17. Mahay, D.; Terenghi, G.; Shawcross, S. G., Schwann cell mediated trophic effects by differentiated mesenchymal stem cells. *Exp. Cell Res.* **2008**, *314*, 2692-701.
18. Mahay, D.; Terenghi, G.; Shawcross, S. G., Growth factors in mesenchymal stem cells following glial-cell differentiation. *Biotechnol. Appl. Biochem.* **2008**, *51*, 167-76.
19. Caddick, J.; Kingham, P. J.; Gardiner, N. J.; Wiberg, M.; Terenghi, G., Phenotypic and functional characteristics of mesenchymal stem cells differentiated along a Schwann cell lineage. *Glia* **2006**, *54*, 840-9.
20. Uz, M.; Das, S. R.; Ding, S.; Sakaguchi, D. S.; Claussen, J. C.; Mallapragada, S. K., Advances in Controlling Differentiation of Adult Stem Cells for Peripheral Nerve Regeneration. *Adv. Healthcare Mater.* **2018**, *7*, 1701046.
21. Scadden, D. T., The stem-cell niche as an entity of action. *Nature* **2006**, *441*, 1075-1079.
22. Keilhoff, G.; Stang, F.; Goihl, A.; Wolf, G.; Fansa, H., Transdifferentiated mesenchymal stem cells as alternative therapy in supporting nerve regeneration and myelination. *Cell. Mol. Neurobiol.* **2006**, *26*, 1235-1252.

- 1
2
3 23. Uz, M.; Buyukoz, M.; Sharma, A. D.; Sakaguchi, D. S.; Altinkaya, S. A.; Mallapragada,
4 S. K., Gelatin-based 3D conduits for transdifferentiation of mesenchymal stem cells into Schwann
5 cell-like phenotypes. *Acta Biomat.* **2017**, *53*, 293-306.
- 6 24. Das, S. R.; Uz, M.; Ding, S.; Lentner, M. T.; Hondred, J. A.; Cargill, A. A.; Sakaguchi, D.
7 S.; Mallapragada, S.; Claussen, J. C., Electrical Differentiation of Mesenchymal Stem Cells into
8 Schwann-Cell-Like Phenotypes Using Inkjet-Printed Graphene Circuits. *Adv. Healthcare Mater.*
9 **2017**, *6*, 1601087.
- 10 25. Sharma, A. D.; Zbarska, S.; Petersen, E. M.; Marti, M. E.; Mallapragada, S. K.; Sakaguchi,
11 D. S., Oriented growth and transdifferentiation of mesenchymal stem cells towards a Schwann cell
12 fate on micropatterned substrates. *J. Biosci. Bioeng.* **2016**, *121*, 325-335.
- 13 26. Ye, E.-A.; Chawla, S. S.; Khan, M. Z.; Sakaguchi, D. S., Bone marrow-derived
14 mesenchymal stem cells (MSCs) stimulate neurite outgrowth from differentiating adult
15 hippocampal progenitor cells. *Stem Cell Biol. Res.* **2016**, *3*, 3.
- 16 27. Iwasaki, Y.; Ishikawa, M.; Okada, N.; Koizumi, S., Induction of a distinct morphology and
17 signal transduction in TrkB/PC12 cells by nerve growth factor and brain-derived neurotrophic
18 factor. *J. Neurochem.* **1997**, *68*, 927-34.
- 19 28. Fraley, S. I.; Feng, Y.; Krishnamurthy, R.; Kim, D.-H.; Celedon, A.; Longmore, G. D.;
20 Wirtz, D., A distinctive role for focal adhesion proteins in three-dimensional cell motility. *Nat.*
21 *Cell Biol.* **2010**, *12*, 598-604.
- 22 29. Harunaga, J. S.; Yamada, K. M., Cell-matrix adhesions in 3D. *Matrix Biol.* **2011**, *30*, 363-
23 368.
- 24 30. Kubow, K. E.; Horwitz, A. R., Reducing background fluorescence reveals adhesions in 3D
25 matrices. *Nat. Cell Biol.* **2011**, *13*, 3-5.
- 26 31. Engler, A. J.; Sen, S.; Sweeney, H. L.; Discher, D. E., Matrix elasticity directs stem cell
27 lineage specification. *Cell* **2006**, *126*, 677-89.
- 28 32. Lanniel, M.; Huq, E.; Allen, S.; Buttery, L.; Williams, P. M.; Alexander, M. R., Substrate
29 induced differentiation of human mesenchymal stem cells on hydrogels with modified surface
30 chemistry and controlled modulus. *Soft Matt.* **2011**, *7*, 6501-6514.
- 31 33. Lee, J. H.; Park, H. K.; Kim, K. S., Intrinsic and extrinsic mechanical properties related to
32 the differentiation of mesenchymal stem cells. *Biochem. Biophys. Res. Comm.* **2015**, *473*, 752-7.
- 33 34. Gonzalez-Martinez, T.; Perez-Pinera, P.; Diaz-Esnal, B.; Vega, J. A., S-100 proteins in the
34 human peripheral nervous system. *Microscopy Res. Tech.* **2003**, *60*, 633-8.
- 35 35. Jessen, K. R.; Mirsky, R., Schwann cells and their precursors emerge as major regulators
36 of nerve development. *Trends Neurosci.* **1999**, *22*, 402-10.
- 37 36. Jessen, K. R.; Mirsky, R., The repair Schwann cell and its function in regenerating nerves.
38 *J. Physiol.* **2016**, *594*, 3521-31.
- 39 37. Guo, W.; Wang, S.; Yu, X.; Qiu, J.; Li, J.; Tang, W.; Li, Z.; Mou, X.; Liu, H.; Wang, Z.,
40 Construction of a 3D rGO-collagen hybrid scaffold for enhancement of the neural differentiation
41 of mesenchymal stem cells. *Nanoscale* **2016**, *8*, 1897-1904.
- 42 38. Kim, T.-H.; Lee, K.-B.; Choi, J.-W., 3D graphene oxide-encapsulated gold nanoparticles
43 to detect neural stem cell differentiation. *Biomater.* **2013**, *34*, 8660-8670.
- 44 39. Lee, Y.-J.; Jang, W.; Im, H.; Sung, J.-S., Extremely low frequency electromagnetic fields
45 enhance neuronal differentiation of human mesenchymal stem cells on graphene-based substrates.
46 *Curr. Appl. Phys.* **2015**, *15*, S95-S102.
- 47
48
49
50
51
52
53
54
55
56
57
58
59
60

40. Park, S. Y.; Park, J.; Sim, S. H.; Sung, M. G.; Kim, K. S.; Hong, B. H.; Hong, S., Enhanced Differentiation of Human Neural Stem Cells into Neurons on Graphene. *Adv. Mater.* **2011**, *23*, H263-H267.
41. Solanki, A.; Chueng, S.-T. D.; Yin, P. T.; Kappera, R.; Chhowalla, M.; Lee, K.-B., Axonal Alignment and Enhanced Neuronal Differentiation of Neural Stem Cells on Graphene-Nanoparticle Hybrid Structures. *Adv. Mater.* **2013**, *25*, 5477-5482.
42. Guo, W.; Zhang, X.; Yu, X.; Wang, S.; Qiu, J.; Tang, W.; Li, L.; Liu, H.; Wang, Z. L., Self-Powered Electrical Stimulation for Enhancing Neural Differentiation of Mesenchymal Stem Cells on Graphene–Poly(3,4-ethylenedioxythiophene) Hybrid Microfibers. *ACS Nano* **2016**, *10*, 5086-5095.
43. Henley, J.; Poo, M.-m., Guiding neuronal growth cones using Ca^{2+} signals. *Trends Cell Biol.* **14**, 320-330.
44. Sheng, L.; Leshchyn'ska, I.; Sytnyk, V., Cell adhesion and intracellular calcium signaling in neurons. *Cell Comm. Signal.* **2013**, *11*, 1-13.
45. Takeichi, M.; Okada, T. S., Roles of magnesium and calcium ions in cell-to-substrate adhesion. *Exp. Cell Res.* **1972**, *74*, 51-60.
46. Park, J.-E.; Seo, Y.-K.; Yoon, H.-H.; Kim, C.-W.; Park, J.-K.; Jeon, S., Electromagnetic fields induce neural differentiation of human bone marrow derived mesenchymal stem cells via ROS mediated EGFR activation. *Neurochem. Int.* **2013**, *62*, 418-424.
47. Hammerick, K. E.; Longaker, M. T.; Prinz, F. B., In vitro effects of direct current electric fields on adipose-derived stromal cells. *Biochem. Biophys. Res. Comm.* **2010**, *397*, 12-17.
48. Thrivikraman, G.; Madras, G.; Basu, B., Intermittent electrical stimuli for guidance of human mesenchymal stem cell lineage commitment towards neural-like cells on electroconductive substrates. *Biomater.* **2014**, *35*, 6219-6235.
49. Schlosshauer, B.; Müller, E.; Schröder, B.; Planck, H.; Müller, H.-W., Rat Schwann cells in bioresorbable nerve guides to promote and accelerate axonal regeneration. *Brain Res.* **2003**, *963*, 321-326.

Table of Contents Graphic

